Title
Enzyme-Responsive Delivery of Multiple Proteins with Spatiotemporal Control

Journal
Advanced Materials, 27(24)

ISSN
0935-9648

Authors
Zhu, S
Nih, L
Carmichael, ST
et al.

Publication Date
2015-06-01

DOI
10.1002/adma.201500417

Peer reviewed

Enzyme-Responsive Delivery of Multiple Proteins with Spatiotemporal Control

Suwei Zhu, Lina Nih, S. Thomas Carmichael, Yunfeng Lu, and Tatiana Segura**

During tissue repair, the orderly presentation of signal proteins in coordination with proteolytic enzymes generally directs the hierarchical remodeling of diseased tissues.[1] For example, angiogenic growth factors in association with tissue-specific protease cascades direct vascular sprouts and subsequent stabilization of blood vessels.[2] In order to deliver multiple signal molecules in a desired sequence, researchers have attempted to develop delivery vehicles with spatiotemporal control by trapping proteins within degradable polymers such as poly(lactide-*co*-glycolic acid), poly(ε-caprolactone), and hydrogels. Representative examples include the composite films made by the layer-by-layer assembly of proteins and polymers,[3] as well as the composite scaffolds made by electrospinning[4] or by fusing polymer particles that contain desired proteins using organic vapor or high-pressure CO_2.[5] For the composite films, the sequential release of the proteins is achieved through a hydrolyzable barrier that separates the layers of the first protein from the subsequent ones; after releasing the first protein, the hydrolysis of the barrier allows for the release of the subsequent proteins. For the composite scaffolds, the sequential release is achieved based on different hydrolysis rates of the polymer moieties within the composites. Although these delivery vehicles enable the sequential elution of multiple proteins, the release process is constitutive which cannot be programmed to respond to any particular biological event. Furthermore, the synthesis of such composites requires harsh chemical processes involving the use of intense mixing and/or organic solvents, which can easily denature growth factors.

Protease-based protein delivery systems were previously studied by others to either directly conjugate proteins to matrices via a protease-sensitive peptide linker or to attach proteins within a bulk hydrogel that is crosslinked by protease-sensitive peptides.[6] However, both approaches expose proteins to the reactive chemical environment, which challenges the stability and bioactivity of proteins.[7] Additionally, these approaches are highly dependent on the number and the type of the functional groups on backbone scaffolds for modifications with different peptide linkers, which limits the applicability of

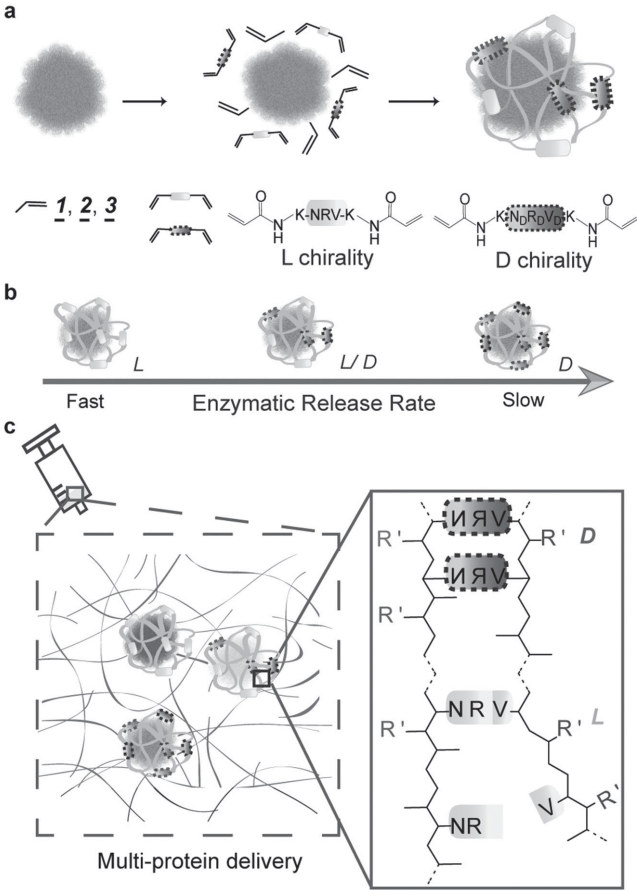

Scheme 1. Illustration of chirality-controlled, enzyme-responsive protein nanocapsules with temporal control. a) The synthesis of the nanocapsules by enriching monomers and crosslinkers around an individual protein molecule and by subsequent in situ polymerization. The monomers can be acrylamide (**1**, neutral), N-(3-aminopropyl)methacrylamide (**2**, positively charged), or 2-acrylamino-2-methyl-1-propanesulfonic acid (**3**, negatively charged). The crosslinkers include a mixture of designed molar ratios of L and D (dashed outline) peptide enantiomers with a sequence of Asn-Arg-Val (substrate of plasmin). b) The rate of enzymatic degradations of individual nanocapsule is tuned by varying the ratio of L to D peptide crosslinkers used: faster with more L peptide, slower with more D peptide. c) Nanocapsules of different proteins and of varying degradation rates can be mixed in matrices (or buffer) of choice for injectable delivery of multiple proteins with precise temporal control in protease-specific disease models.

S. Zhu, Dr. L. Nih, Prof. Y. Lu, Prof. T. Segura
Department of Chemical and Biomolecular Engineering
University of California
Los Angeles, 420 Westwood Plaza
Los Angeles, CA 90095, USA
E-mail: luucla@ucla.edu;
tsegura@ucla.edu
Prof. S. T. Carmichael
Department of Neurology
David Geffen School of Medicine
University of California
Los Angeles, 710 Westwood Plaza
Los Angeles, CA 90095, USA

DOI: 10.1002/adma.201500417

multiple proteins with temporal release control and the variety for the selection of buffers or matrices.

We have developed a platform technology for protein delivery based on a mild encapsulation process, in which individual whole proteins are wrapped within an in situ formed thin polymer shell.[8] Since the spatial and temporal patterns of protease expressions are closely related to pathophysiological states,[9] incorporating protease-specific and cleavable peptides within the polymer shells allows for disease-state-specific delivery of signal molecules. Here, we investigated the peptide substrates made from the L or the D chiral form of amino acids and found that they exhibited similar chemical specificity but distinct proteolytic kinetics (i.e., ≈10-fold slower for D enantiomer than the L enantiomer, Supporting Information, Table S1). Thus by controlling the L to D ratios of peptide crosslinkers within the shells, the delivery of multiple proteins with spatiotemporal control in response to the proteolytic enzymes in diseased sites could be achieved.

Scheme 1a illustrates our design using plasmin-sensitive peptides as labile crosslinkers. Driven by non-covalent interactions, monomers with neutral **1**, positive **2**, or negative **3** charges, as well as peptide crosslinkers, are spontaneously enriched around protein molecules. Free-radical polymerization gradually grows a nanogel shell around each protein, leading to the formation of protease-responsive nanocapsules denoted as n(Protein)$_{x\%}$, where protein denotes the protein core and *x*% denotes the molar percentage of L peptide in the total L+D peptide crosslinkers used for the nanogel shell (Scheme 1a). Increasing the ratio of L crosslinker (*x*%, fast degrading rate) leads to nanocapsules with a faster release kinetic, while

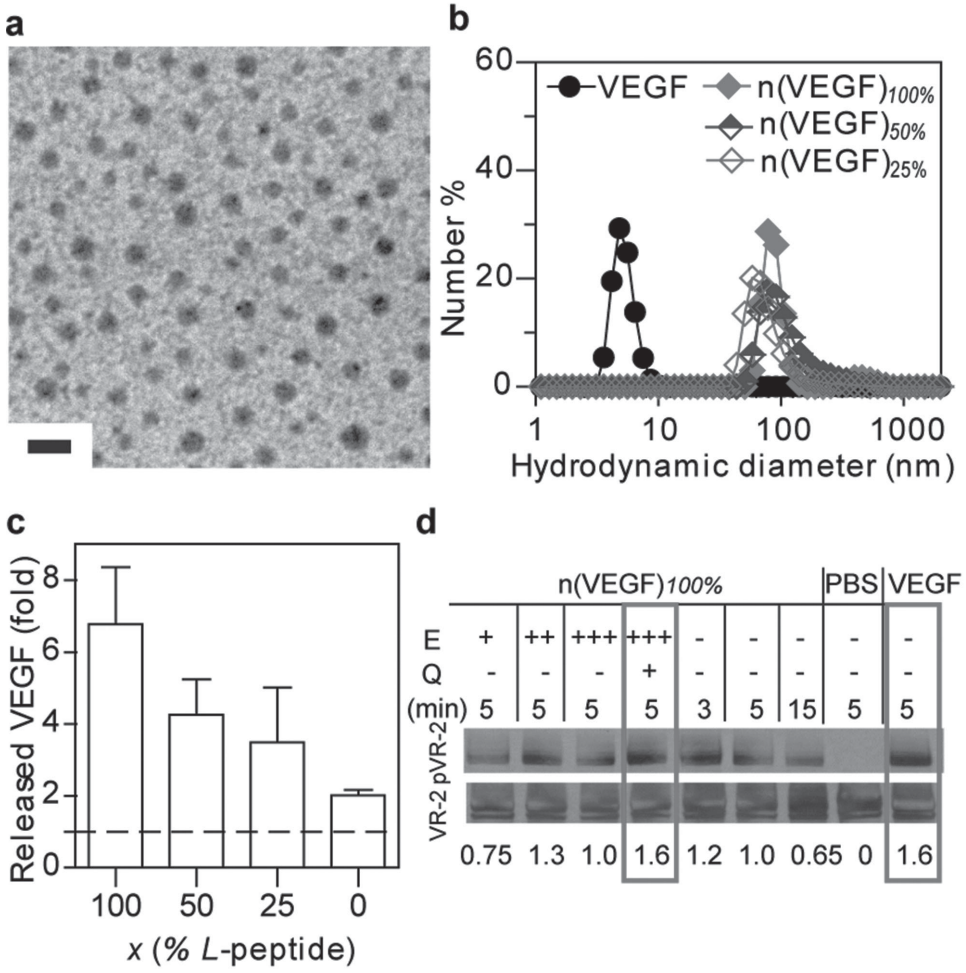

Figure 1. Characterizations of protein nanocapsules. a) A transmission electron microscopic image of nanocapsules synthesized with gold nanoparticle (AuNP) (4 nm)-labeled VEGF. AuNP was stained using a silver enhancer kit to exhibit as dark black dots within the gray spheres of n(VEGF-AuNP)$_{100\%}$ (scale bar 100 nm). b) The hydrodynamic sizes of n(VEGF) of different L-to-D ratios via dynamic light scattering. c) Incubating n(VEGF)$_{100\%}$, n(VEGF)$_{50\%}$, n(VEGF)$_{25\%}$, or n(VEGF)$_{0\%}$ with plasmin for 20 min in ELISA measured the in vitro enzymatic release rates of nanocapsules. d) Western blotting analysis of the activity of encapsulated VEGF showed that it remained identical to free VEGF in inducing receptor phosphorylation. The encapsulated VEGF was first released from n(VEGF)$_{100\%}$ at 50 ng mL^{-1} via the incubation with an enzyme (E), trypsin, at increasing mass ratios of trypsin:n(VEGF)$_{100\%}$ = 0.05:1 (labeled as E+), 0.1:1 (labeled as E++), and 0.2:1 (labeled as E+++). To prevent the released VEGF from being degraded, an inhibitor, aprotinin, was subsequently used to quench (Q) the excessive proteolytic activity of trypsin. Released VEGF, as well as n(VEGF)$_{100\%}$ without enzyme pretreatment and free VEGF (50 ng mL^{-1}) were incubated with serum-starved human vein endothelial cells for specified amounts of time (min). The activity was indicated by the normalized intensity of the phosphorylation of VEGF receptor-2 (pVR-2) to total VEGF receptor-2 (VR-2).

Adv. Mater. **2015**,
DOI: 10.1002/adma.201500417

decreasing L percentage results in slower releasable nanocapsules (Scheme 1b). Upon protease degradation of the shell of nanocapsules, the released protein can exert its normal biological function. The degraded nanogel fragments – charged polyacrylamide segments with cleaved peptides – are expected to be biocompatible in the biological milieu, as previously observed for similar polymers.[10] Furthermore, such nanocapsules can be homogeneously dispersed within an injectable hydrogel, providing an injectable delivery platform for enhanced wound healing and tissue repair (Scheme 1c).

As an example, nanocapsules containing vascular endothelial growth factor-A 165 (VEGF), designated as n(VEGF)$_{100\%}$, were synthesized using **1** and **2** as the co-monomer and 100% plasmin-labile L-peptide as the crosslinker. These nanocapsules displayed a spherical morphology and by labeling VEGF molecules with gold nanoparticles, each nanocapsule was found to contain one to two VEGF molecules (**Figure 1**a). Nanocapsules synthesized with different ratios of enantiomeric peptides, including n(VEGF)$_{100\%}$, n(VEGF)$_{50\%}$, and n(VEGF)$_{25\%}$, exhibited similar hydrodynamic diameters, indicating an unbiased polymerization activity between the L and D peptide crosslinkers (Figure 1b). Furthermore, nanocapsules of platelet derived growth factor-BB (PDGF), denoted as n(PDGF)$_{100\%}$, were also synthesized with the nanogel shell being polymerized by **1** and **3** as the co-monomer and 100% L peptide as the crosslinker, which also display a similar nanoscale size under transmission electron microscopy (TEM) (Figure S1, Supporting Information). The plasmin-responsive release capability of the nanocapsule vehicles features a programmable release rate. Figure 1c compares the amount of VEGF released from n(VEGF)$_{100\%}$, n(VEGF)$_{50\%}$, n(VEGF)$_{25\%}$, and n(VEGF)$_{0\%}$ after the incubation with plasmin for 20 min. While a sixfold increase of VEGF was observed in n(VEGF)$_{100\%}$ after plasmin incubation, there was only a one-fold increase in the quantity of VEGF with n(VEGF)$_{0\%}$, confirming that decreasing the L-peptide content within the shells leads to decreasing in vitro release rates. The activity of encapsulated proteins is protected and can be released by isolated enzymes or cell-secreted proteases. To demonstrate these two approaches, first, the degradation of nanocapsules was triggered by an isolated protease, trypsin, followed by a protease inhibitor to quench subsequent proteolytic degradation; thus, the released VEGF was able to induce the phosphorylation of cell-surface receptors to the same extent as a free protein did (Figure 1d). This result suggests that 100% of the encapsulated proteins can be retrieved with appropriate amounts of enzymes and that the encapsulated proteins retain 100% of its activity. Second, cells can mediate the release of proteins from nanocapsules with the proteolytic and fibrinolytic proenzymes[11] secreted by cells. We incubated n(PDGF)$_{100\%}$, n(PDGF)$_{0\%}$, and free PDGF with human dermal fibroblasts and observed some degree of receptor phosphorylation induced by nanocapsules (Figure S2, Supporting Information), which indicated that some degree of encapsulated protein was released from n(PDGF)$_{100\%}$ in the time-frame tested.

Therapeutic angiogenesis in vivo, a crucial process toward wound healing, requires the continuous presence of VEGF, which is subject to a narrow therapeutic window.[12] However the frequent re-dosing of high concentrations of VEGF (tens of micrograms) to wound beds has been the standard practice due to inevitable passive leaching of naked proteins from conventional scaffolds and matrices.[13] Here, we tested the ability of n(VEGF)$_{100\%}$/n(VEGF)$_{25\%}$ mixture (100 ng each, 200 ng combined) to promote vascularization in a challenging environment: the avascular stroke cavity. VEGF is one of the candidate molecules used in poststroke neural repair therapies to enhance angiogenesis and functional recovery. However, the delivery of VEGF to ischemic brains is often complicated by the induction of disordered vasculature.[14] Immunohistological analysis of glucose transporter 1 (highly expressed in the brain endothelium) and PDGF receptor-β (highly expressed in pericytes) showed that the bolus delivery of free VEGF within a hyaluronic acid (HA) hydrogel did not improve the level of vascularization compared to HA hydrogel alone. In contrast, the n(VEGF)$_{100\%}$/n(VEGF)$_{25\%}$ mixture led to statistically significant increases in vascularization and pericyte coverage in both the infarct (inside the stroke cavity) as well as peri-infarct (surrounding the stroke) regions (**Figure 2**). This result confirms that the nanocapsules are responsive to brain wound environments to allow for active VEGF release at a rate and level sufficient for enhanced vascularization.

In addition to achieving the temporal control of one protein release in response to proteases, the nanocapsule technology

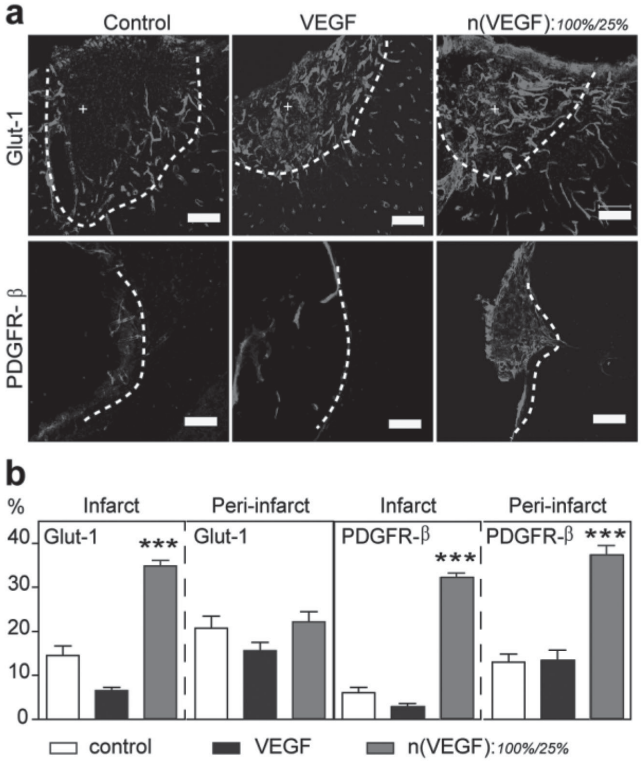

Figure 2. Temporal control of VEGF delivery in mouse stroke model. a) Representative confocal images of blood vessels (Glut-1+) and their maturity markers (PDGFR-β+) in the infarct (indicated by +) and peri-infarct areas of stroke (separated by the dashed line). The stroke was treated with in situ crosslinked, adhesion peptide-modified hyaluronic acid hydrogel containing no VEGF (control), unencapsulated free VEGF (200 ng), or n(VEGF)$_{100\%}$: n(VEGF)$_{25\%}$ at 100 ng : 100 ng. b) Analysis of Glut-1 and PDGFR-β markers for the vascularization in the infarct and peri-infarct areas of stroke. (ANOVA with Tukey's post test, mean ± SEM, N = 3–4, *p < 0.05, **p < 0.01, ***p < 0.001.) Scale bar = 100 μm.

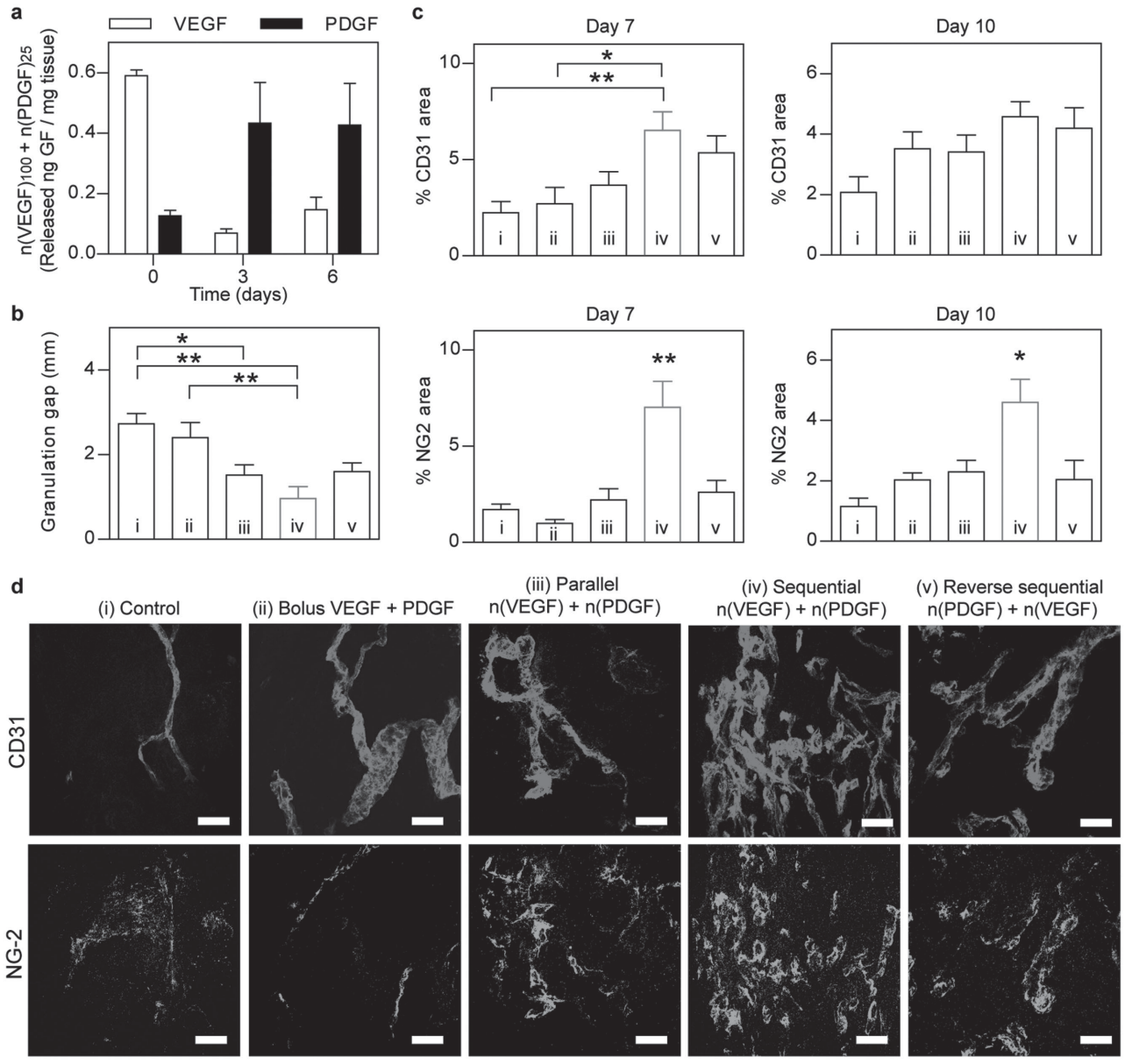

Figure 3. In vivo co-delivery of VEGF and PDGF with temporal control in diabetic mouse skin wounds. a) Tissue-ELISA analysis of wound-mediated release of proteins from $n(VEGF)_{100\%}$ and $n(PDGF)_{25\%}$ at day 0, 3, and 6 post surgery in normal balb/c mice. b) Quantification of the gap of granulation tissues in diabetic skin wounds at day 7 in db/db mice. Wound was dressed with fibrin matrices that contained (i) no growth factors (control), (ii) unencapsulated free VEGF (200 ng) and PDGF (200 ng), (iii) mixture of $n(VEGF)_{100\%}/n(VEGF)_{25\%}/n(PDGF)_{100\%}/n(PDGF)_{25\%}$ at 100 ng/100 ng/100 ng/100 ng (parallel), (iv) mixture of $n(VEGF)_{100\%}/n(VEGF)_{25\%}/n(PDGF)_{25\%}/n(PDGF)_{10\%}$ at 100 ng/100 ng/100 ng/100 ng (sequential), and (v) mixture of $n(VEGF)_{25\%}/n(VEGF)_{10\%}/n(PDGF)_{100\%}/n(PDGF)_{25\%}$ at 100 ng/100 ng/100 ng/100 ng (reverse sequential). c) Immunohistochemical analysis of vessel endothelium (CD31+) and pericyte coverage (NG2+) at day 7 and 10. d) Representative confocal images of CD31 (upper row) and NG2 (lower row) in the granulation tissue of diabetic skin wounds at day 7 (ANOVA with Tukey's post test, mean ± SEM, $N = 4–6$, $*p < 0.05$, $**p < 0.01$.) Scale bar = 50 μm (d).

also enables sequential delivery of multiple proteins by using mixed nanocapsules made with designed protein cores, as well as the types and ratios of L/D crosslinkers. **Figure 3**a shows that the release profile of $n(VEGF)_{100\%}$ and $n(PDGF)_{25\%}$ co-delivered to skin wounds from the same scaffold. As expected, VEGF was detected between 0 and 3 days and PDGF was detected between 3 and 6 days, demonstrating the sequential release (Figure 3a, Figure S3, Supporting Information). Specifically, $n(VEGF)_{100\%}$ led to an excess of 200 pg VEGF per mg of tissue than endogenous VEGF at day 0, yet no significant difference on day 3 or 6, suggesting that $n(VEGF)_{100\%}$ was mostly released by day 3 since urokinase plasminogen activator is initially activated in wounds and subsequently deactivated as wound heals and decreases in size.[15] However with the incorporation of D chiral peptide, the excess of PDGF detected with $n(PDGF)_{25\%}$ on day 3 and 6 further demonstrated in vivo delayed release enabled by

Adv. Mater. 2015,
DOI: 10.1002/adma.201500417

chiral protein nanocapsules. Such time scales are relevant for angiogenesis in mouse skin wounds where the angiogenic peak occurs at 3–5 d.

To further analyze the ability of using enantiomeric nanocapsules to achieve sequential release of growth factors, we sought to demonstrate with the well-documented synergistic effects of VEGF and PDGF[5a] in inducing pericyte coverage of nascent blood vessels in a diabetic skin wound healing model.[16] Because impaired wound closure in diabetic patients is correlated with impaired angiogenesis and angiogenesis is correlated with the ability to sustain granulation tissue, we compared the formation of granulation tissue and the related angiogenesis process. The nanocapsule mixture of $n(VEGF)_{100\%}$/$n(VEGF)_{25\%}$/$n(PDGF)_{25\%}$/$n(PDGF)_{10\%}$ comprised a sequential delivery strategy of VEGF followed by PDGF, whereas $n(VEGF)_{25\%}$/$n(VEGF)_{10\%}$/$n(PDGF)_{100\%}$/$n(PDGF)_{25\%}$ formed the reverse sequence of PDGF release followed by VEGF. Among the two sequential, parallel and bolus delivery strategies, only the sequentially released VEGF then PDGF (condition iv in Figure 3 and Figure S4, Supporting Information) led to enhanced formation of granulation tissue and an increased vessel density with pericyte coverage. This observation further confirms that these chirally different nanocapsules can be engineered to release proteins in multiphases in a wound environment. In contrast, nanocapsules that released both VEGF and PDGF in parallel (condition iii in Figure 3) did not show enhanced angiogenesis or mature blood vessels. Interestingly, we observed a non-significant difference in the CD31 expression between wounds treated with the reverse sequential strategy (PDGF first then VEGF, condition v) and the orthogonal sequential delivery (VEGF first then PDGF condition iv), on which a recent report could possibly shed some light where the angiogenesis process in mouse bone healing was promoted by increasing the PDGF secretion from preosteoclasts or by a treatment with exogenous PDGF.[17] Nevertheless, the reverse sequential strategy failed to promote pericyte coverage in our study. This last example further exemplifies the ability to control protein release rates with nanocapsules at disease sites.

In conclusion, we have designed a general platform for multiprotein delivery with spatiotemporal definitions based on enantiomerically engineered protein nanocapsules. Peptide chirality is for the first time utilized to modulate the enzymatic release of proteins and, enabled by the nanocapsule technology, to achieve spatiotemporal control of multiple proteins in cell-instructed microenvironments. These nanocapsules are facilely formed, robust, and applicable to proteins in general, providing highly effective protein therapeutic vehicles for disease-specific tissue engineering and regenerative medicine.

Experimental Section

Synthesis of Protein Nanocapsules: The nanocapsules were synthesized using in situ free-radical polymerization. To synthesize n(VEGF), VEGF was diluted in a buffer solution of 10×10^{-3} M sodium bicarbonate (pH = 8.55) at a final reaction concentration of 100 μg mL^{-1}. Acrylamide (AAM) and *N*-(3-aminopropyl)methacrylamide (APM) and crosslinkers (bisacrylated L/D-KNRVK, or methylene bisacrylamide) were subsequently added to the protein solution (at the molar ratio of VEGF:AAM:APM:crosslinker = 1:3000:3000:600). To synthesize n(PDGF), PDGF was diluted in phosphate buffer saline (PBS) (pH = 7.2–7.4) at a final reaction concentration of 100 μg mL^{-1}. Acrylamide, 2-acrylamino-2-methyl-1-propanesulfonic acid (AAMPS), and crosslinkers (bisacrylated L/D-KNVRK) were subsequently added to the protein solution (at the molar ratio of PDGF:AAM:AAMPS:crosslinker = 1:1500:4500:600). Then, freshly prepared ammonium persulfate (APS) (at a molar ratio of Protein:APS = 1:745) and tetramethylethylenediamine (TEMED) (at a molar ratio of Protein:TEMED = 1:45000) were added to initiate in situ polymerization to form the nanocapsules. The reaction was carried out under inert gas for 2–4 hours at 4 °C. The mixture was purified by dialysis against 10×10^{-3} M phosphate buffer (pH ≈7.0). Systemic studies, including size, morphology and structure of the nanocapsules, enzymatic kinetics, cell studies, and animal models (tissue enzyme-linked immunosorbent assay (ELISA), focal and permanent stroke model and impaired wound healing in diabetic mice) were carried out to demonstrate the delivery platform, which are detailed in the Supporting Information.

Supporting Information

Supporting Information is available from the Wiley Online Library or from the author.

Acknowledgements

The authors thank Angela Wong, an undergraduate researcher, and Eric Lin, a high school researcher, for their hard work. The authors would also like to thank the Electron Imaging Center for NanoMachines supported by NIH (1S10RR23057 to ZHZ) and the California NanoSystems Institute (CNSI) for the use of instruments. This project was supported by the American Heart Association under Grant No. 11GRNT7630021AHA, the National Institutes of Health (NIH) under Grant Nos. R01HL110592 and R01NS079691, and NSF IGERT: Materials Creation Training Program (MCTP) – DGE-0654431. Author contributions: S.Z. and L.N. performed the experiments; S.Z., L.N., S.T.C., Y.L., and T.S. designed the experiments; S.Z., L.N., and T.S. analyzed the results. S.Z., Y.L., and T.S. wrote the manuscript, with inputs from all authors. Animal procedures were performed in accordance with the US National Institutes of Health Animal Protection Guidelines and the University of California Los Angeles Chancellor's Animal Research Committee.

Received: January 26, 2015
Revised: April 10, 2015
Published online:

[1] B. Leader, Q. J. Baca, D. E. Golan, *Nat. Rev. Drug Discovery* **2008**, *7*, 21.
[2] a) G. C. Gurtner, S. Werner, Y. Barrandon, M. T. Longaker, *Nature* **2008**, *453*, 314; b) R. D. Sinclair, T. J. Ryan, *Aus. J. Dermatol.* **1994**, *35*, 35.
[3] B. B. Hsu, K. S. Jamieson, S. R. Hagerman, E. Holler, J. Y. Ljubimova, P. T. Hammond, *Angew. Chem. Int. Ed. Engl.* **2014**, *53*, 8093.
[4] A. K. Ekaputra, G. D. Prestwich, S. M. Cool, D. W. Hutmacher, *Biomaterials* **2011**, *32*, 8108.
[5] a) T. P. Richardson, M. C. Peters, A. B. Ennett, D. J. Mooney, *Nat. Biotechnol.* **2001**, *19*, 1029; b) Y. Wang, M. J. Cooke, N. Sachewsky, C. M. Morshead, M. S. Shoichet, *J. Controlled Release* **2013**, *172*, 1.
[6] D. Seliktar, A. H. Zisch, M. P. Lutolf, J. L. Wrana, J. A. Hubbell, *J. Biomed. Mater. Res. A* **2004**, *68*, 704.
[7] a) J. Wen, S. M. Anderson, J. J. Du, M. Yan, J. Wang, M. Q. Shen, Y. F. Lu, T. Segura, *Adv. Mater.* **2011**, *23*, 4549; b) B. Q. Shen,

K. Xu, L. Liu, H. Raab, S. Bhakta, M. Kenrick, K. L. Parsons-Reponte, J. Tien, S. F. Yu, E. Mai, D. Li, J. Tibbitts, J. Baudys, O. M. Saad, S. J. Scales, P. J. McDonald, P. E. Hass, C. Eigenbrot, T. Nguyen, W. A. Solis, R. N. Fuji, K. M. Flagella, D. Patel, S. D. Spencer, L. A. Khawli, A. Ebens, W. L. Wong, R. Vandlen, S. Kaur, M. X. Sliwkowski, R. H. Scheller, P. Polakis, J. R. Junutula, *Nat. Biotechnol.* **2012**, *30*, 184.

[8] M. Yan, J. Du, Z. Gu, M. Liang, Y. Hu, W. Zhang, S. Priceman, L. Wu, H. Zhou, Z. Liu, T. Segura, Y. Tang, Y. Lu, *Nat. Nanotechnol.* **2009**, *5*, 48.

[9] T. N. Demidova-Rice, M. R. Hamblin, I. M. Herman, *Adv. Skin Wound Care* **2012**, *25*, 349.

[10] M. C. Darnell, J. Y. Sun, M. Mehta, C. Johnson, P. R. Arany, Z. Suo, D. J. Mooney, *Biomaterials* **2013**, *34*, 8042.

[11] J. C. Zhang, J. Wojta, B. R. Binder, *J. Thorac. Cardiovasc. Surg.* **1995**, *109*, 1059.

[12] a) C. R. Ozawa, A. Banfi, N. L. Glazer, G. Thurston, M. L. Springer, P. E. Kraft, D. M. McDonald, H. M. Blau, *J. Clin. Invest.* **2004**, *113*, 516; b) G. von Degenfeld, A. Banfi, M. L. Springer, R. A. Wagner, J. Jacobi, C. R. Ozawa, M. J. Merchant, J. P. Cooke, H. M. Blau, *FASEB J.* **2006**, *20*, 2657.

[13] a) R. D. Galiano, O. M. Tepper, C. R. Pelo, K. A. Bhatt, M. Callaghan, N. Bastidas, S. Bunting, H. G. Steinmetz, G. C. Gurtner, *Am. J. Pathol.* **2004**, *164*, 1935; b) D. G. Greenhalgh, K. H. Sprugel, M. J. Murray, R. Ross, *Am. J. Pathol.* **1990**, *136*, 1235.

[14] a) Z. G. Zhang, L. Zhang, Q. Jiang, R. Zhang, K. Davies, C. Powers, N. Bruggen, M. Chopp, *J. Clin. Invest.* **2000**, *106*, 829; b) Y. Ma, A. Zechariah, Y. Qu, D. M. Hermann, *J. Neurosci. Res.* **2012**, *90*, 1873.

[15] A. B. Wysocki, A. O. Kusakabe, S. Chang, T. L. Tuan, *Wound Repair Regen.* **1999**, *7*, 154.

[16] S. Frank, G. Hubner, G. Breier, M. T. Longaker, D. G. Greenhalgh, S. Werner, *J. Biol. Chem.* **1995**, *270*, 12607.

[17] H. Xie, Z. Cui, L. Wang, Z. Xia, Y. Hu, L. Xian, C. Li, L. Xie, J. Crane, M. Wan, G. Zhen, Q. Bian, B. Yu, W. Chang, T. Qiu, M. Pickarski, T. Duong le, J. J. Windle, X. Luo, E. Liao, X. Cao, *Nat. Med.* **2014**, *20*, 1270.

Adv. Mater. **2015**,
DOI: 10.1002/adma.201500417